Heat Transfer of Three-Dimensional Backward-Facing Step Flow -Local Heat Transfer Coefficients on the Bottom Wall and Upper Wall

Shuai ZOU*, Takeshi MURAYAMA*, Shogo MOTODA*, Shumpei HARA, Kyoji INAOKA*****

(Received April 27, 2020)

The heat transfer mechanism especially three-dimensional characteristics based on backward-facing step (BFS) flow mounted in a duct under relative low Reynolds number region have not yet clearly clarified by experimental measurement. Thermo-sensitive liquid crystal method was made use of for obtaining the local heat transfer distributions on the bottom wall and upper wall to investigate the local heat transfer deterioration and enhancement area and check the existence of three-dimensionality. MLP (Multilayer Perceptron) method was adopted for building the relationship between the RGB value of thermo-sensitive liquid crystal sheets and wall temperature value. Large attention was paid to the average and maximum Nusselt number on the bottom wall and upper wall. The average Nusselt number value over the entire bottom wall and the upper wall can be estimated by the average Nusselt number at the center of the flow channel. Obvious heat transfer three-dimensionality was found both on the bottom wall and upper wall in low Reynolds number range.

Key words : backward-facing step, three-dimensional flow, upper wall, bottom wall, heat transfer

1. Introduction

Backward-facing step (BFS) flow which was applied to many heat exchanging devices was introduced as a basic model that involves the most important features of a separated and reattachment flow [1]. As is summarized in the review study of Chen et al. [2], early studies [3, 4] mainly focused on theoretical models and experiments for reattachment length, friction, pressure variations. The aspect ratio of the stepped duct in most studies was set large and the spanwise direction of the flow path was set sufficiently. However, in practical applications, the flow channel is thought to be a duct having sidewalls and upper walls, which cannot be ignored. Since the three-dimensional feature of the flow has been observed [5], new investigations focusing on the three-dimensional flow structures have been started and some useful results have been obtained. Iwai et al. [6] have carried out the three-dimensional numerical computation changing the channel aspect ratios from 4 to 24 for the laminar flow regime. It was revealed that the existence of sidewall intensively affects the flow and thermal fields downstream the step and showed unique heat transfer distribution on the bottom wall. Intensive efforts have also been made by Nie and Armaly using numerical and experimental methods. The aspect ratio was set to be 8 and reported that near the sidewall, the jet-like flow impinges on the bottom wall from the step and causes the maximum local heat transfer there [7]. Inaoka et al. [8] revealed that the flow reattachment region of the 3D duct case is quite different from that of the 2D case. Some

*Department of Mechanical Engineering, Faculty of Science and Engineering, Doshisha University, Kyoto
Telephone: +81-0807-857-3389, Email: doctorshuaizou@gmail.com
**Department of Mechanical Engineering, Faculty of Science and Engineering, Doshisha University, Kyoto
Telephone: +81-774-65-6832, Email: shhara@mail.doshisha.ac.jp
***Department of Mechanical Engineering, Faculty of Science and Engineering, Doshisha University, Kyoto
Telephone: +81-0774-65-6463, Email: kinaoka@mail.doshisha.ac.jp

numerical predictions reported that 3D effects would become important when $Re > 500$ [9, 10], under low Re number conditions, and the 3D effects will become largely limited while the universal structure under high Re may dominant the flow after the step. However, the comparison between prediction and experiments does not agree well with each other in low Reynolds number range, due to boundary and three-dimensional effects. According to the review report of Chen et al. [2], the thermal effects on the BFS flow separation, evolution of coherent structures and reattachment process, which are very important as for real applications, have rarely been discussed, there are not many experimental studies on heat transfer aspect, as the heating region (global or local) becomes more complicated. Experiments are mainly conducted in the high Re region, while numerical studies are mainly focused on the relatively low Re region.

To sum up, three-dimensional heat transfer characteristics of backward-facing step flow in a duct at low Reynolds number should be clarified. To realize this purpose, in detail, the average Nu and maximum Nu, the ratio of maximum Nu over the entire wall to that in the duct centerline should be investigated on the bottom wall and upper wall for a wide variety of the flow Reynolds number is low Reynolds number range (Re=400-900).

2. Experimental Apparatus and Procedures

2.1 *Experimental apparatus*

In this experiment, an experimental device using water as the working fluid was adopted. Figure 1 shows a schematic diagram of the experimental apparatus. The rigorous design of the circulating water tank ensures that the water flowing into the test section is fully developed laminar flow. Figure 2 shows the test section which is a rectangular duct with a width W_D = 240 mm and a height H = 30 mm, and a step with a height S = 15 mm was mounted inside. The aspect ratio of the upstream entrance was 16, and the expansion ratio was 2. The Reynolds number is defined by the step height S as the representative length. The origin of the coordinate axis is at the center of the bottom line in the spanwise direction. The x-axis represents flow direction, the y-axis represents step height direction, and the z-axis represents a spanwise direction.

2.2 *Heat transfer experiment procedure*

Thermal measurements were conducted on the bottom wall and the upper wall of the BFS model, respectively. Since the heat transfer measurement method of the upper wall is the same as that of the bottom wall surface, here, the bottom wall representing the upper wall is utilized to describe the heat transfer experiment procedure. As shown in Fig. 3, stainless steel foil was applied to the entire bottom wall for 31S length in the streamwise direction, the inner surface of the bottom plate was covered with thin stainless-steel foil strips of 47.2 mm wide, 470 mm long and 20 μm thick, having 1 mm spanwise spacing with each other. These foil strips were connected electrically in series and were heated by passing an alternating current through them, a constant heat flux heating condition was established at the wall. Heat conduction loss toward the outside of the duct was neglected since its value was less than 0.3% of the total heat flux [1]. The liquid crystal sheet of 75 μm thick was glued between the heater strips and the transparent bottom wall to monitor the local distributions of the bottom wall temperature [1]. The color distribution of a thermo-sensitive liquid crystal sheet (RW20-25 manufactured by Nippon Capsule Products Co., Ltd.) attached to the bottom wall surface of the stainless-steel foil was photographed by a CMOS camera (Nikon D7000) through a transparent acrylic bottom wall. As shown in Fig. 4, the relative luminance values of R, G and B colors were obtained from the acquired images, and the local wall temperature was obtained using MLP (Multilayer Perceptron) method [2]. The local heat transfer coefficient h was calculated by dividing constant heat flux q_w by the difference between the wall temperature

and the bulk temperature along the streamwise direction.

$$h = \frac{q_w}{T_w - T_m} \quad (1)$$

where *Tw* is the local wall temperature and *Tm* is the bulk temperature along the streamwise direction. The constant wall heat flux q_w was calculated from the electric power input through the stainless foil strips. To evaluate the local heat transfer characteristics in the following discussion, the local *Nu* defined based on the step height *S* as Eq. (2) will be used.

$$Nu = \frac{hS}{\lambda} \quad (2)$$

where λ is the thermal conductivity of the fluid, the reference length is set by step height.

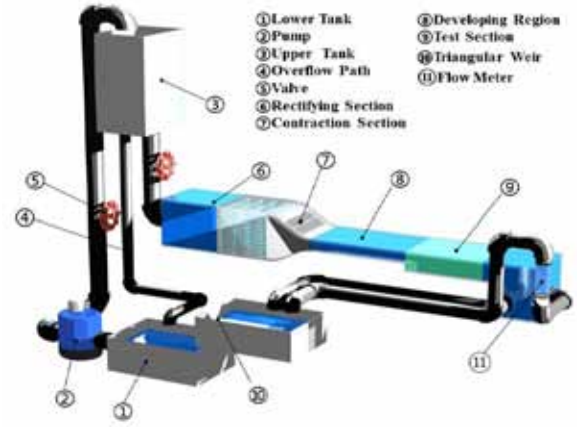

Fig. 1. Closed water channel used in the present study flow in a duct.

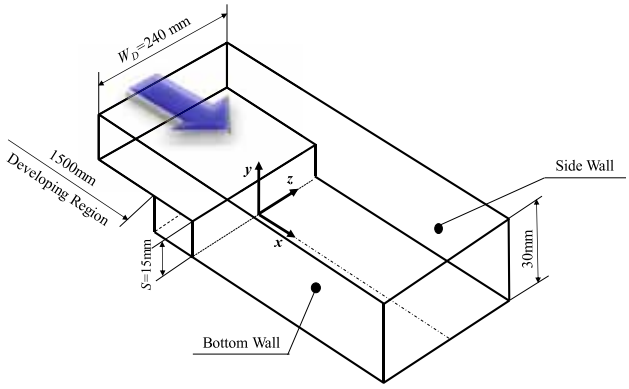

Fig. 2. Test section of a backward-facing step flow.

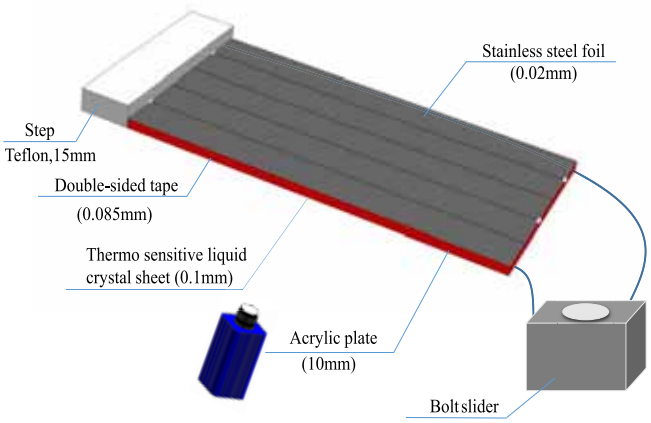

Fig. 3. Illustration of the heat transfer experiment.

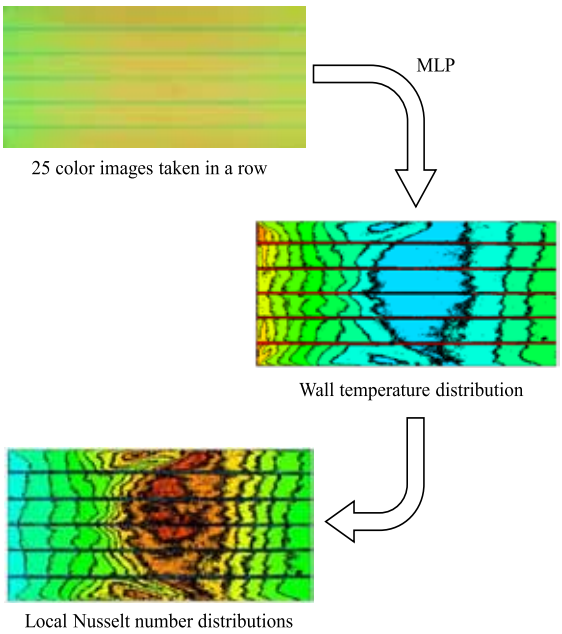

Fig. 4. Measurement of the heat transfer coefficient using MLP method.

To verify the precision of MLP method and reliability of liquid crystal method, validation experiments were done in advance in the normal parallel flow, and the *Nu* distribution along the center line on the bottom wall was compared with theoretical value, the relative error after *x*/*S*=3.3 was 4.8%. Then the heat transfer experiments were done on the bottom wall and upper wall respectively (Fig. 5 (b), Fig. 5 (c)).

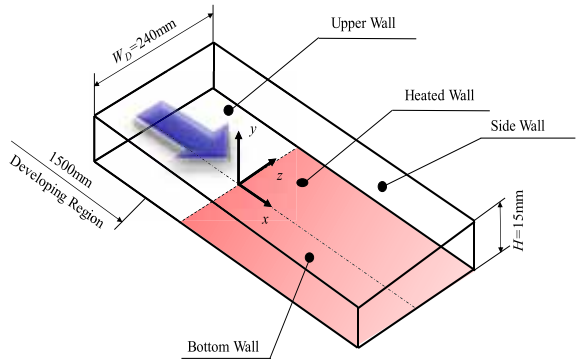

(a) Bottom wall heated for parallel plated flow case

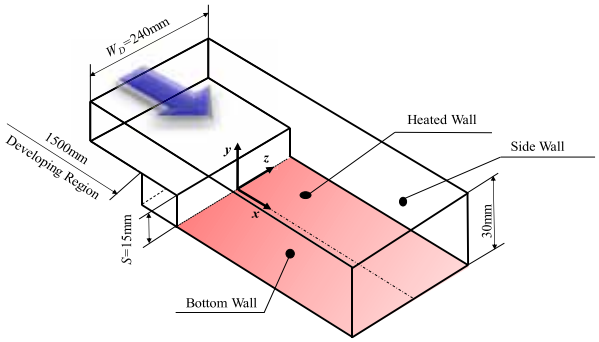

(b) Bottom wall heated for stepped flow case

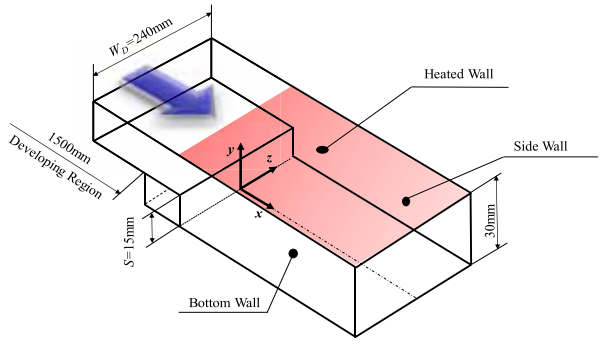

(c) Upper wall heated for stepped flow case

Fig. 5. Heat transfer measurement setup.

3. Results and Discussion

3.1 *Distributions of heat transfer coefficient on the bottom wall*

Figure 6 shows the distribution of the local *Nu* on the bottom wall for the representative Reynolds numbers (400, 600, 900), x-coordinate represents the flow direction and z-coordinate represents the spanwise direction. z/W_D=0 represents the center and z/W_D=0.5 represents sidewall. The contour is integrated with x_u-line extracted by PIV experiments. As mentioned by Nie and Armaly et al., x_u-line is a collection of a series of points along the spanwise direction where the wall shear stress is equal to zero [11, 12], which is used to delineate the recirculation zone along the spanwise direction. For all cases, a large heat transfer deterioration area is generated just behind the step and before x_u-line, and increases along the streamwise direction then decrease after the peak value. The maximum *Nu* value appears near the sidewall. From the aspect of the flow direction, there is a spatial lag in the position where the *Nu* is relatively high compared to the reattachment position. In the low Reynolds number range, the heat transfer distribution is similar to that in the research of Iwai et al., and Nie & Armaly. The shape of the x_u-line is like that of the *Nu* contour boundary. At the superimposed diagram of the velocity fluctuation intensity, average velocity vector, and reattachment position of Reynolds number 400, 900 shown in Fig. 7, pay attention to the vicinity of the sidewall, there is a strong reverse flow region upstream from the flow center, the flow region and high heat

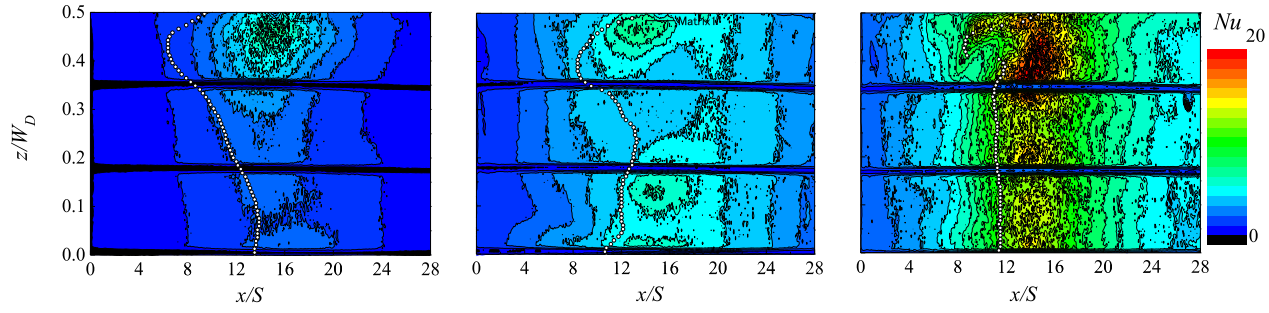

(a) *Re*=400 (b) *Re*=600 (c) *Re*=900

Fig. 6. Distribution of the local Nusselt number on the bottom wall.

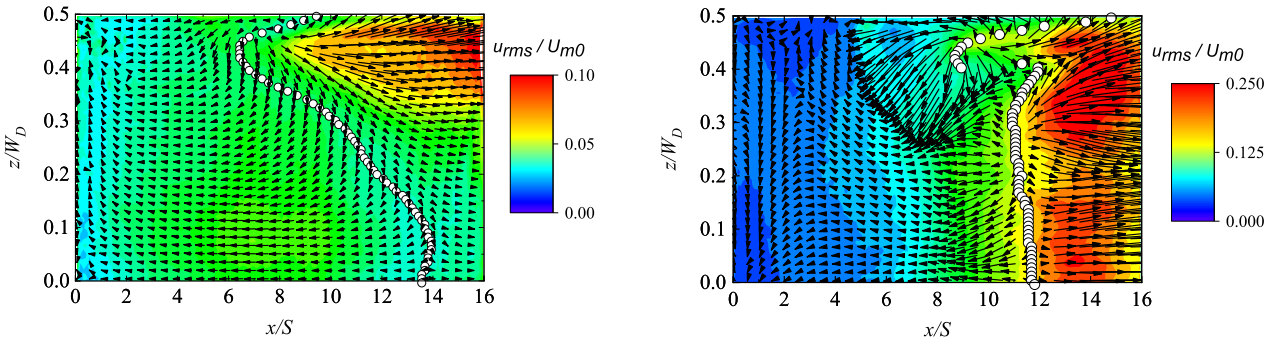

(a) *Re*=400 (b) *Re*=900

Fig. 7. Velocity fluctuation intensity distribution on the bottom wall.

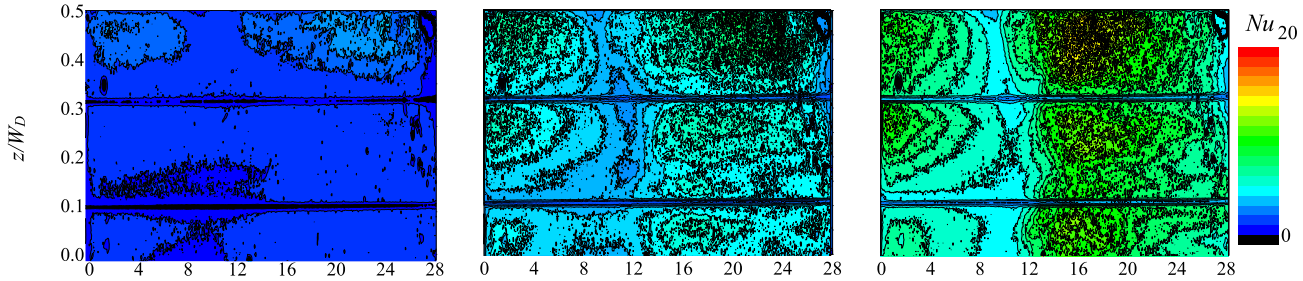

(a) *Re*=400 (b) *Re*=600 (c) *Re*=900

Fig. 8. Distribution of the local Nusselt number on the upper wall for the representative Reynolds number cases.

transfer coefficient region are in good agreement, the velocity fluctuation intensity here is high and on the downstream side of x_u-line. The maximum heat transfer distribution area is consistent with the region where the flow fluctuation intensity is the highest, revealing that the heat transfer promotion has a close relationship to the turbulence of flow there.

3.2 *Distributions of heat transfer coefficient on the upper wall*

Same as the coordinates setting of the bottom wall，Fig. 8 shows the *Nu* distribution on the upper wall for the representative Reynolds numbers (*Re*=400, 600, 900). The changing trend of the *Nu* distribution along the flow path on the upper wall surface is not consistent with that on the bottom wall surface. The area where the heat transfer deteriorates is no longer adjacent to the step but in a specific narrow area downstream.

3.3 *Comparison of heat transfer coefficient on the bottom wall and upper wall*

Figure 9 shows the average *Nu* over the entire bottom wall Nu_{bave} and upper wall Nu_{upave}, and the average *Nu* at the centerline of the bottom wall Nu_{bcave} and upper wall Nu_{upcave} at different Reynolds numbers. Here, the channel length for doing average was 31*S*. The black and blue plots show the experimental results obtained at Reynolds number less than 1000, and the red plot shows the results of previous experimental research of Inaoka et al. From this figure, it can be seen that both Nu_{bcave} and Nu_{bave} are smoothly linked to the previous results and that the average heat transfer increases significantly up to *Re* = 1000 with the increase of Reynolds number, and then increases relatively slowly thereafter. On the upper wall, the increasing tendency even values are almost the same as that on the bottom wall. For all cases, the values of Nu_{ave} and Nu_{cave} are almost the same in all regions of the ds number. From this, it can be said that when considering the range of 31*S'* downstream of the flow channel, the average *Nu* of the entire bottom wall and the upper wall

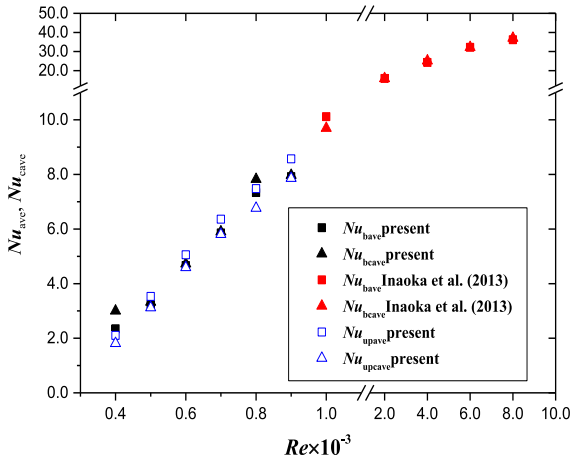

Fig. 9. Nu_{ave} and Nu_{cave} in different Re.

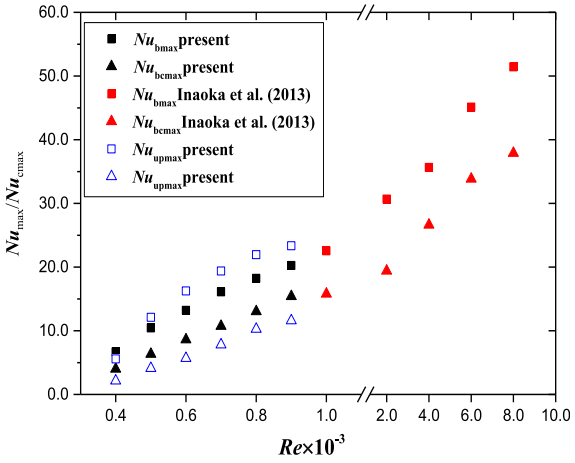

Fig. 10. Nu_{max} and Nu_{cmax} in different Re.

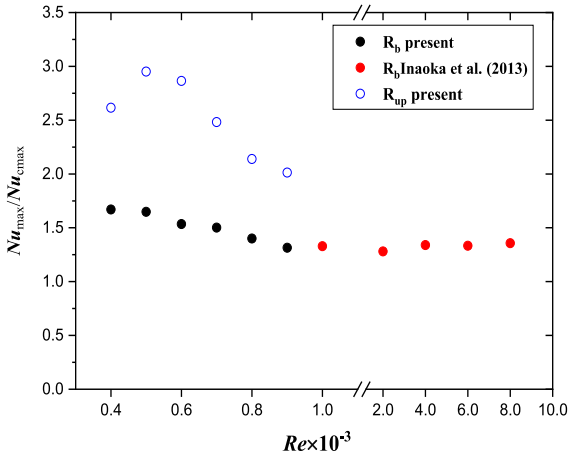

Fig. 11. Variation of the ratio of Nu_{max} to Nu_{cmax} for Re.

can be estimated by the average Nu at the center of the flow channel. Figure 10 shows the maximum Nu over the entire bottom wall Nu_{bmax} and upper wall Nu_{bcmax}, and the maximum Nu at the centerline of the bottom wall Nu_{bcmax} and upper wall Nu_{upcmax} at different Reynolds numbers. Figure 11 shows the ratio between the two in Fig. 10. The black and blue plots in each figure show the results of the present experiment, and the red plots show the results of Inaoka et al. From Fig. 10, both values increase with the increase of Reynolds number. As for the present experimental results, Nu_{cmax} has linear change not only on the bottom wall but also on the upper wall. It is worth noting that the discrepancies between Nu_{upmax} and Nu_{upcmax} are larger than those between Nu_{bmax} and Nu_{bcmax}. From Fig. 11, on the bottom wall, after Re = 1000, the ratio value is around 1.3 and does not change much even if the Reynolds number increases. On the other hand, in the region below Re = 1000, the ratio value increases as the Reynolds number decreases. The fact that all the ratios are over 1 indicates non-uniform heat transfer distribution in the spanwise direction exists on the bottom wall, when Re=400, the non-uniform intensity is strongest. On the upper wall, the ratio is much higher than that of the bottom wall, indicating the higher effect by the flow three-dimensionality occurs there, especially around relative low Reynolds number range (400, 500, 600).

4. Summary

Heat transfer measurements were done on the bottom and upper wall of the BFS flow in a duct in a relatively low Reynolds number range (Re=400-900). From the perspective of heat transfer distribution, it is summarized that this flow model has three-dimensional characteristics and intensively affects the heat transfer distribution on the walls. The specific conclusions are as follows:

(1) When considering the range of 31S downstream of the flow channel, the average Nu value over the entire bottom wall or upper wall can be estimated by averaging that at its center line in the Reynolds number range from 400 to 900.

(2) On the bottom wall, the area where heat transfer is enhanced and deteriorated is mainly distributed downstream of the step and near the sidewall, respectively. Flow disturbances play a leading role in heat transfer enhancement. The ratio of Nu_{max} to Nu_{cmax} in different Re on the bottom wall proves the existence of a three-dimensional feature of this fluid flow model. The three-dimensional flow effect is most obvious at approximately Re=400.

(3) On the upper wall, the ratio of Nu_{max} to Nu_{cmax} in different Re also reveals that the three-dimensional flow effects heat transfer characteristics of the upper wall. Furthermore, the three-dimensional characteristics there is stronger than that of the bottom wall in the same Reynolds number condition.

References

1) J. H. Xu, S. Zou, K. Inaoka, and G. N. Xi, “Effect of Reynolds Number on Flow and Heat Transfer in Incompressible Forced Convection over a 3D Backward-Facing Step”, *Int. J. Refrig.,* **79**, 164-175 (2017).
2) L. Chen, K. Asai, T. Nonomura, G. Xi, and T. Liu, “A Review of Backward-Facing Step (BFS) Flow Mechanisms, Heat Transfer and Control”, *Therm. Sci. Eng. Prog.,* **6**, 194-216 (2018).
3) E. W. Adams, and J. K. Eaton, “An LDA Study of the Backward-Facing Step Flow, Including the Effects of Velocity Bias”, *J. Fluids Eng.,* **110**[3], 275-282 (1988).
4) B. F. Armaly, F. Durst, J. Pereira, and B. Schönung, “Experimental and Theoretical Investigation of Backward-Facing Step Flow”, *J. Fluid Mech.,* **127**, 473-496 (1983).
5) G. Papadopoulos, and M. V. O¨tu¨gen, “Separating and Reattaching Flow Structure in a Suddenly Expanding Rectangular Duct”, *J. Fluids Eng.,* **117**[1], 17-23 (1995).
6) H. Iwai, K. Nakabe, and K. Suzuki, “Flow and Heat Transfer Characteristics of Backward-Facing Step Laminar Flow in a Rectangular Duct”, *Int. J. Heat Mass Transfer,* **43**[3], 457-471 (2000).
7) J. H. Nie, and B. F. Armaly, “Three-Dimensional Convective Flow Adjacent to Backward-Facing Step-Effects of Step Height”, *Int. J. Heat Mass Transfer,* **45**[12], 2431-2438 (2002).
8) K. Inaoka, and M. Senda, “Heat Transfer and Fluid Flow Characteristics of a Backward-Facing Step Flow in a Duct”, *Transactions of the Japan Society of Mechanical Engineers Series B,* **79**[804], 1651-1663 (2013).
9) L. Kaiktsis, G. E. Karniadakis, and S. A. Orszag, “Onset of Three-Dimensionality, Equilibria, and Early Transition in Flow over a Backward-Facing Step”, *J. Fluid Mech.,* **231**, 501-528 (1991).
10) E. Steinthorsson, M.-S. Liou, L. A. Povinelli, and A. Arnone, “Numerical Simulations of Three-Dimensional Laminar Flow over a Backward Facing Step; Flow near Side Walls”. *ASME Fluids Engineering Division, Summer Conf.*, Washington, D.C. (1993)
11) J. G. Barbosa-Saldaña, and N. Anand, “Flow over a Three-Dimensional Horizontal Forward-Facing Step”, *Numer. Heat Transfer, Part A,* **53**[1], 1-17 (2007).
12) J. H. Nie, and B. F. Armaly, “Reattachment of Three-Dimensional Flow Adjacent to Backward-Facing Step”, *J. Heat Transfer,* **125**[3], 422-428 (2003).